11

Flow cytometric characterization and sorting of ultrasound contrast agents

Maja Mujić[1], Spiros Kotopoulis[2,3], Anthony Delalande[1,3] Marianne Enger[1], Odd Helge Gilja[1,2] Emmet Mc Cormack[1], Michiel Postema[3], Bjørn Tore Gjertsen[1,4]

[1]Institute of Medicine, Hematology Section, University of Bergen, Bergen, Norway,
[2]National Centre for Ultrasound in Gastroenterology, Haukeland University Hospital, Bergen, Norway,
[3]Department of Physics and Technology, University of Bergen, Norway,
[4]Department of Internal Medicine, Hematology Section, Haukeland University Hospital, Bergen, Norway

Abstract

Ultrasound contrast agents consist of microscopically small gas bubbles encapsulated by elastic shells, and are regularly employed in ultrasound blood pool perfusion diagnostics and currently explored as drug delivery vehicles. Successful development of functional ultrasound contrast imaging demands precise and effective microbubble evaluation techniques. We have examined flow cytometry as a method for *in vitro* quantification, optical characterization and sorting of microbubbles with flexible lipid shell or albumin shell. Flow cytometry provided reproducible side and forward scatter analysis and quantification of gas filled microbubbles enumeration, at various pressure levels and fluid flow speeds. Quantification allowed determination of the static microbubble stability, indicating increased stability at 4°C compared with storage at ambient temperature. Flow cytometry allowed detection of microbubbles in mixture with cell lines or whole blood *ex vivo*. Furthermore, flow cytometry analysis permitted microbubble sorting by size or fluorescence, allowing evaluation of isolated

microbubble populations. We anticipate that flow cytometry will be a reliable technology for analysis of novel modified microbubbles for use in clinical ultrasonography.

Introduction

Ultrasonography is a cost-effective and safe clinical imaging modality [1]. Blood perfusion imaging is desirable in human diagnostics, but blood is a poor ultrasonic scatterer. Hence, ultrasound contrast agents have been added to the blood pool to increase the signal-to-noise ratio [2,3]. These ultrasound contrast agents consist of liquids containing encapsulated microbubbles. Upon sonication these microbubbles undergo volumetric oscillations [4] resulting in a detectable acoustic signal. Potential therapeutic applications of ultrasound contrast agents include ultrasound guided sonothrombolysis [5], molecular imaging [6,7], and drug and gene delivery [8-14].

The microbubble oscillations create a transient permeabilization of cell membranes enhancing drug uptake [15]. This microbubble-induced permeabilization may be the consequence of pore formation in the cell membrane [16-19], thus leading to targeted delivery of therapeutic agents [11,20].

Recently we have found that fluorescence-labelled microbubbles can be forced/pushed into cancerous cells using clinical diagnostic settings allowing the delivery of a therapeutic payload [19]. This delivery is primarily dependant on the acoustic conditions the microbubble size distribution and shell composition. Thus, using microbubbles loaded with specific agents could enhance the release of the therapeutic agent at a desired location.

In all applications of clinical ultrasound it is critical to select microbubbles with specific sizes or composition [21]. Current sizing methods include Coulter counting, zeta sizing and optical microscopy, although none of these methods allow for microbubble sorting. Current size sorting methods include filtration and using microfluidics chambers, whilst atomic force microscopy can be used to characterize the microbubble shell properties [22]. None of these methods allow for real time multi-parameter sizing and sorting, and have limitations for use in medium or high throughput chemical screens of microbubble shell modification. For further development of therapeutic and diagnostic ultrasound contrast agents, there is a need for a reliable methodology to size, select and sort microbubbles. Here, we present data that suggest that both low threshold and state-of-the-art flow cytometry instrumentation represent versatile and simple technology platforms for future development of ultrasound contrast agents.

Flow cytometry is a well–established method used in clinical practice and biomedical research to characterize cells [23,24]. We hypothesize that flow cytometry can be used to non-destructively size, select and sort ultrasound contrast agent microbubbles in real-time.

Materials and methods

Cell lines and whole blood

Human acute myeloid leukaemia cell lines NB4 and HL-60 were purchased from Deutsche Sammlung von Mikroorganismen und Zellkulturen GmbH (Braunschweig, Germany). MOLM-13 and MV4-11 cell lines were purchased from ATCC subsidiary LGC Standards AB (Borås, Sweden). NB5, HL-60 and MOLM-13 were cultured in RPMI-1640 medium (Sigma, St. Louis, MO) with 10% FBS, 2 mM L-glutamine and Penicillin (50 U mL^{-1})/Streptomycin (50 U mL^{-1}) (Gibco, Grand Island, NY). The MV4-11 cell line cultured in IMDM (BioWhittaker, Cambrex Bio Science, Verviers, Belgium) with 10% FBS, L-glutamine and Penicillin/Streptomycin. Human whole blood samples were collected from healthy volunteers.

Microscopy

A TE2000 fluorescence microscope (Nikon Corporation, Tokyo, Japan) was used with Hoffman modulation contrast for microscopy of microbubbles. The microbubbles were placed on an object slide and imaged at room temperature using a 40×/0.55 HMC LWD air objective. For detection of DiI fluorescence a Leica TCS SP2 AOBS inverted confocal microscope (Leica Microsystems, Heidelberg, Germany), with a 63×/1.40 HCX PL Apo oil objective and a Helium/Neon I, 1-mW / 543-nm laser was used. A Zeiss LSM 510 META (Carl Zeiss Microscopy AG, Oberkochen, Germany) with a 63×/1.40 Plan-Apochromat oil objective and a Helium/Neon II, 5-mW / 633-nm laser was used to detect DiD fluorescence.

Flow cytometry

Five different flow cytometers were used to analyse the SonoVue® ultrasound contrast agent (Bracco Diagnostics Inc., Milano, Italy): a FACSCalibur using a 12-60 µL/min flow rate at 31 kPa, a FACSAria cell sorter (Becton Dickinson Immunocytometry Systems, San Jose, CA) using a 12-48 µL/min flow rate at 138 kPa, a Cytomics FC 500 (Beckman Coulter Inc., Fullerton, CA) using a 12-60 µL/min flow rate at 207 kPa, an Accuri (Accuri Cytometers, Inc., Ann Arbor, MI) using a 14-66 µL/min flow rate and a non-pressurized system, and a Guava® easyCyte™ 6-2L Base System (Merck Millipore Billerica, MA) using a 60 µL/min flow rate at 55 kPa. In our experiments 2×10^4 microbubbles were analysed for each measurement. FlowJo software version 8.8.6 and 7.6.3 (Tree Star Inc., Ashland, OR) were used to analyze the flow cytometry data.

Microbubble static stability determination

The microbubble static stability was determined by measuring the microbubble concentration using flow cytometry. To determine the microbubble concentration 100 µL of a size and concentration standard (10µm diameter, 1×10^6 fluorospheres/mL) (Flow-Count fluorospheres, Beckman Coulter Inc., Fullerton, CA) were added to 25 µL of each microbubble sample. The concentration of microbubbles was determined using:

$$MC = (\Sigma_{MB}/\Sigma_{FS}) \times FC, \qquad (1)$$

where *MC* is the microbubble concentration, Σ_{MB} is the sum of microbubbles counted, Σ_{FS} is the sum of fluorospheres counted and *FC* is the fluorospheres concentration. Before flow cytometric analysis, microbubbles were counted using a Bürker cell counting chamber (Hawskley, Lancing, United Kingdom). The microbubble stability was measured at stepped time intervals during storage at room temperature (20ºC) or at 4ºC for 96 hours.

Detection of microbubbles in cell lines and whole blood

A volume of 0.5, 1, 10 or 50 µL of microbubbles at a concentration of 0.3×10^6 microbubbles/µL was added to 50 µL of either HL-60, NB4, MOLM-13 or MV4-11 cells (5×10^6/mL) and analyzed using the FACSCalibur flow cytometer. In addition 0.1–50 µL of microbubbles (0.3×10^6 microbubbles/µL) were added to 500 µL whole blood and analyzed by FACSCalibur.

Flow cytometric analysis of SonoVue® and Quantison™ ultrasound contrast agents

The Accuri flow cytometer was used to analyse SonoVue® (Bracco Diagnostics Inc) and Quantison™ (Upperton Limited, Nottingham, UK) ultrasound contrast agents; both individually and in mixture. In addition to the 10-µm size standard a drop of 5.1 µm (5.0–5.9 µm) SPHERO™ COMPtrol Goat anti-Mouse Ig blank (Spherotec Inc., Lake Forest, Illinois) standard particles were used to evaluate the size of SonoVue®.

Fluorescent labeling of microbubbles

To create fluorescent microbubbles, the lipophilic probes DiI (λ_{ex}=549 nm, λ_{em}=565 nm) and DiD (λ_{ex}=644 nm, λ_{em}=665 nm) (Vybrant™ Molecular Probes, Invitrogen, San Diego CA) were added at different concentrations (0.2–12.5 µM) to microbubbles. The same concentrations of DiI were added to NaCl in control experiments.

Fluorescence-activated cell sorting and isolation of microbubbles

The FACSAria cell sorter was used to sort two populations of microbubbles based on their size and fluorescence. For size sorting small and large microbubbles were gated on the FSC-SSC plot. For fluorescence measurements the microbubbles were labelled with DiI or DiD. The system was kept at 4°C at all times to increase the stability of microbubbles. After sorting, both populations were analysed by microscopy and flow cytometry to evaluate the microbubbles presence, the size of the sorted microbubbles, and their fluorescence. Before sorting, microbubble labelling was confirmed by confocal microscopy. A final concentration of 6.25 µM of DiI or DiD was added to microbubbles and sorted using the FACSAria flow cytometer. The fluorescent positive and negative populations were collected after sorting. BD FACSDiva™ software (Becton Dickinson Immunocytometry Systems) was used to draw gates for sorting of microbubbles.

Size distribution, acoustic activity and stability of sorted microbubbles

To measure the microbubble size distribution and to verify if the SonoVue® microbubbles were still acoustically active after sorting, the sorted microbubbles were inserted into an OptiCell® cell culture chamber (Nunc GmbH & Co. KG, Langenselbold,

Germany) filled with 10 mL of 0.9% saline solution. The OptiCell® was placed in the *xy* stage of a TS100 Eclipse inverted microscope (Nikon Corporation, Shinjuku, Tokyo, Japan) and the microbubbles were observed through a 20×/0.40 and 40×/0.55 (Nikon Corporation) objectives. The color charge coupled device (CCD) of a Photron FastCam MC-2.1 high-speed camera (VKT Video Kommunikation GmbH, Pfullingen, Germany) was connected to the microscope via the c-mount and used to capture still images of the sorted microbubbles. The captured images were size calibrated using a Bürker haemocytometer. The acoustic activity and stability of the microbubbles under sonication was checked before and after sorting inside an OptiCell®. To check if the microbubbles were acoustically active a VScan clinical ultrasound scanner (General Electric Healthcare, Fairfield, CT) was used as the ultrasound source. Eco Supergel ultrasound gel (Ceracarta, Forli, Italy) was used to create an acoustic path from the transducer to the OptiCell®. The scanner pointed at the microscope objective and was placed at an elevation angle of 45º and an azimuth of 90º. In all recordings the direction of the sound field is from far right to far left of the frame. The scanner was set at a Mechanical Index of 1.2 and a Thermal Index of 0.4 with colour Doppler activated to allow for the highest possible duty cycle. The acoustic microbubble attraction was monitored using the high-speed camera at 1000 frames per second (25). To measure the size distribution a total of 1328 microbubbles were measured using ImageJ v1.440 (National Institutes of Health, Bethesda, MD).

Statistical analysis

In all figures values are presented as mean ± SEM. Data was compared using an unpaired, two-tailed Student *t*-test. The difference between two samples was considered statistically significant when *p*-value was lower than 0.05. Analyses were performed using GraphPad® Prism 5.0 (GraphPad Software, La Jolla, CA).

Results

Flow cytometry analysis of gas filled microbubbles

To investigate if gas filled microbubbles could be detected by flow cytometry, microbubbles were analysed on multiple flow cytometers of various specifications. Optical microscopy showed microbubble size distribution within the expected size range of 1-10 μm (Fig. 1A). The flow cytometry data showed a specific serpentine pattern on five different flow cytometers when examined for forward and side light scatter (Fig. 1B–F). The serpentine distribution was reproducible independent of the flow cytometer, the fluidic pressure and flow rate (Fig. 1 B-F).

Temperature dependent microbubble stability

The microbubble concentration is proportional to the stability (Fig. 2), thus minimal decay in concentration indicates higher stability. The microbubbles showed equal stability over two hours independent of storage conditions. From 6 to 96 hours when storing at room temperature, the microbubble concentration decreased by a factor of 7 (from 1.84×10^8 microbubbles/mL to 2.7×10^7 microbubbles/mL). In contrast, when

storing at 4ºC, the microbubble concentration was much more stable for up to 48 hours, and a slow decay was seen up to 96 hours (from 2.15×10^8 microbubbles/mL after 6 hours to 1.39×10^8 microbubbles/mL after 96 hours). The microbubble stability at 4ºC was statistically significantly higher when compared to that at room temperature from 24 hours onwards (2.06×10^8 microbubbles/mL versus 1.18×10^8 microbubbles/mL, *p*-value: 0.032).
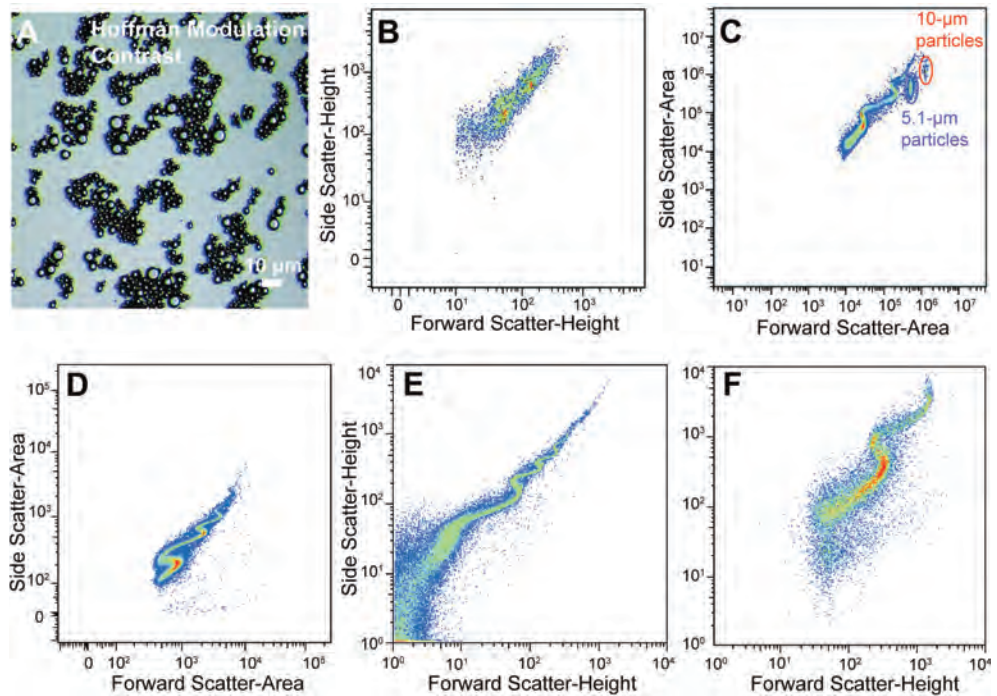

Figure 1 - Micrographs and flow cytometric plots of gas filled soft shell microbubbles. (**A**) Hoffman Modulation contrast (40x HMC LWD air objective) was used for microscopy of microbubbles. Microbubbles (SonoVue®) vary in size between 1-10 µm. Scale bar, 10 µm. (**B**) Flow cytometric analysis of microbubbles using a low-pressure fluidic system, Guava, n=1. (**C**) Flow cytometric analysis of microbubbles with a 10 µm and 5.1 µm standard using a flow cytometers with a low-pressure fluidic system (Accuri), n=10. (**D**) Flow cytometric analysis of microbubbles using a pressurized system, FACS Aria cell sorter, n=10; (**E**) FACS Calibur, n=10; (**F**) Cytomics FC 500, n=2.

Comparing flow cytometry and haemocytometer based concentration measurements of microbubbles, the flow cytometer measured 7% less microbubbles/mL than optical microscopy (3.03×10^8 microbubbles/mL versus 3.28×10^8 microbubbles/mL respectively).
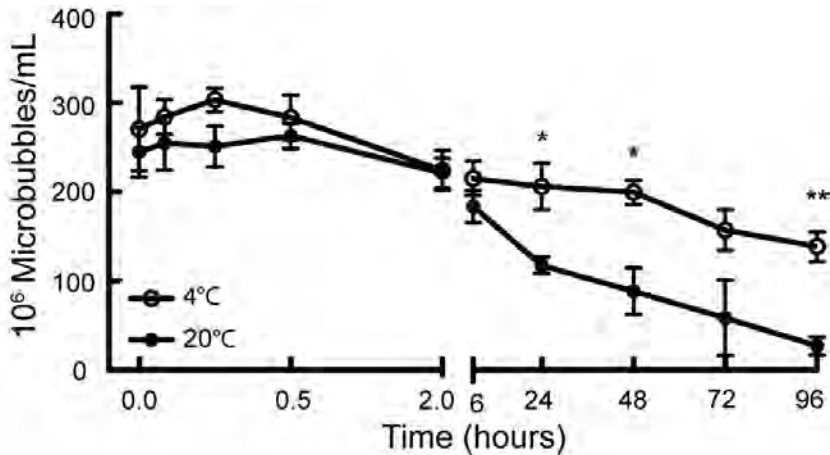
Figure 2- Temperature dependent stability of gas filled microbubbles. The number of microbubbles was determined using the 10 μm size and concentration bead standard. Analyses were done using FACSCalibur. The effect of the two storage conditions; room temperature and 4 °C was determined at selected time points up to 96 hours, n=3. The p value at 24 hours is p=0.0323, at 48 hours is p=0.0197, at 96 hours is p=0.0045. Data are compared using an unpaired, two-tailed Student t test.

Detection of microbubbles in cell lines and whole blood

Differentiating microbubbles within a cell mixture could help validate microbubble cell interactions. This could help improve ultrasound-guided drug delivery. We were able to detect microbubbles in mixture with four different human cell lines, illustrated here by HL-60 acute myeloid leukaemia cells (Fig. 3A). The serpentine shape did not change when microbubbles were mixed with cells. The microbubbles and the cells could be clearly distinguished. Furthermore, we tested if microbubbles were distinguishable in whole blood (Figs. 3B and 3C), a much more complex fluid with multiple cell populations. It was possible to detect the microbubbles at concentrations down to 1:1000 microbubbles to whole blood. The microbubble were stable for up to 60 min in whole blood independent of concentration (Fig. 3D).
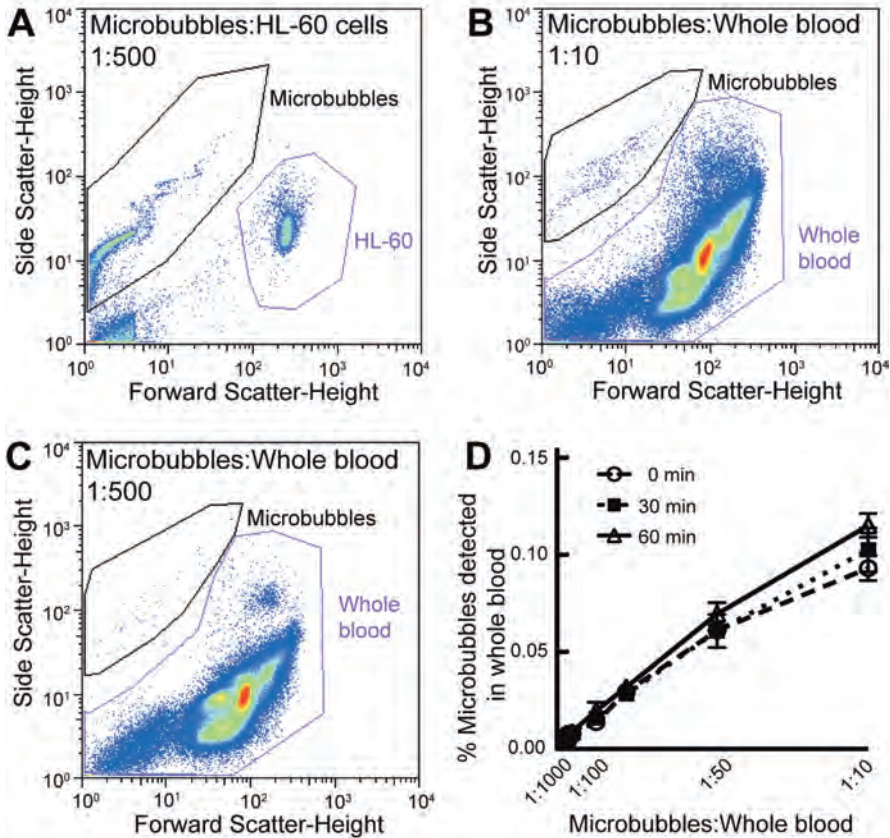
Figure 3 - Discrimination of Microbubbles from mixtures in human cell lines and whole blood. (**A**) Flow cytometric analysis showing microbubbles and the HL-60 leukemic cell line. Similar data was obtained with other human cell lines (microbubble volume : cells volume, 1 : 500, n=3). (**B**) Flow cytometric analysis of microbubbles and whole blood, microbubble volume : whole blood volume - 1 : 10, n=3; (**C**) 1 : 500, n=3. (**D**) Per cent (%) detectable microbubbles in whole blood is indicated at 0, 30 and 60 min, n=3.

Flow cytometric comparison of lipid-shelled (SonoVue®) and albumin-shelled (Quantison™) ultrasound contrast agents

Flow cytometry analysis of the albumin-shelled microbubbles was also possible under the same parameters (Fig. 4A). The scatter pattern was different compared to lipid-shelled ultrasound contrast agent (SonoVue®). The characteristic serpentine shape observed in the lipid-shelled microbubbles was not found in the albumin-shelled microbubbles. In a mixture containing both ultrasound contrast agents, we were able to

distinguish the respective agents (Fig. 4B). This indicates that microbubbles with different shell materials and thus properties could be characterized using flow cytometry
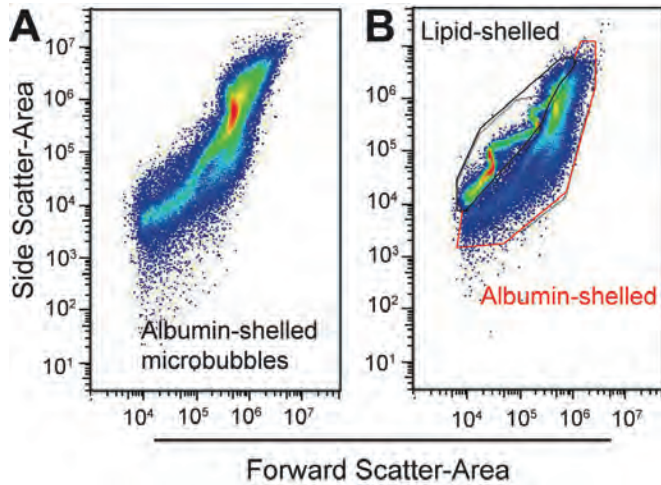

Figure 4 - Flow cytometric analysis of gas filled lipid and albumin microbubbles. (**A**) Flow cytometric analysis of albumin (Quantison™) microbubbles. (**B**) Flow cytometry analysis of combined lipid microbubbles and albumin microbubbles.

Fluorescence-activated cell sorting and isolation of intact microbubbles

Sorting of microbubbles based on size is useful as small diameter microbubbles with a narrow size distribution have the ability to pass through small capillaries [27], and be used to improve harmonic imaging [21,26]. The unsorted microbubbles showed a Gaussian type distribution with a mean diameter of 3.49±2.05 µm (Fig. 5A). The small-sorted microbubbles also showed a Gaussian distribution with a mean diameter of 2.82±0.77 µm (Fig. 5B). The mean diameter of the large-sorted microbubbles was 5.96±2.54 µm, the histogram indicated two peaks, one at 8.3 µm containing large microbubbles, and one at 3.0 µm containing smaller microbubbles (Fig. 5C). The size distribution parameters of the three populations clearly demonstrate that smaller bubbles had a narrow size distribution and could be easily separated whilst the larger population contained a large amount of smaller bubble contaminates (Fig. 5D). Both populations were seen to still be acoustically active after sorting. The physical properties of intact microbubbles were tested after sorting by acoustic attraction (Fig. 5E). The sorted microbubbles were attracted to each other and coalesce (fuse into one entity) after 235 milliseconds of low energy ultrasound indicating they are still acoustically active and oscillating in phase, similarly to unsorted microbubbles prepared freshly (data not shown). Confocal microscopy confirmed DiI and DiD labelling on the lipid shell of the microbubbles (Fig. 6A and 6C respectively). An increase in mean fluorescence intensity was observed with increasing concentration of the fluorescent

dye as illustrated by DiI (Fig. 6B). The highest fluorescence intensity was obtained at an optimal dye concentration of 6.25 μM, with only a small difference in fluorescence compared to 12.5 μM. Additionally, the mean fluorescence intensity increased over time and incubation of microbubbles with DiI for 90 min resulted in the highest mean fluorescence intensity for the various concentrations of the dye. Fluorescence-based sorting could be used to select labelled microbubbles for use in ultrasound-assisted drug delivery or in molecular imaging. Sorting of microbubbles resulted in a significant increase in the amount of fluorescently labelled microbubbles after sorting (Fig. 6D; from 9.9% before to 65.6% after). The population that was sorted for non-fluorescent microbubbles contained only 5.3% DiD positive microbubbles confirming successful sorting of fluorescence-labelled microbubbles.
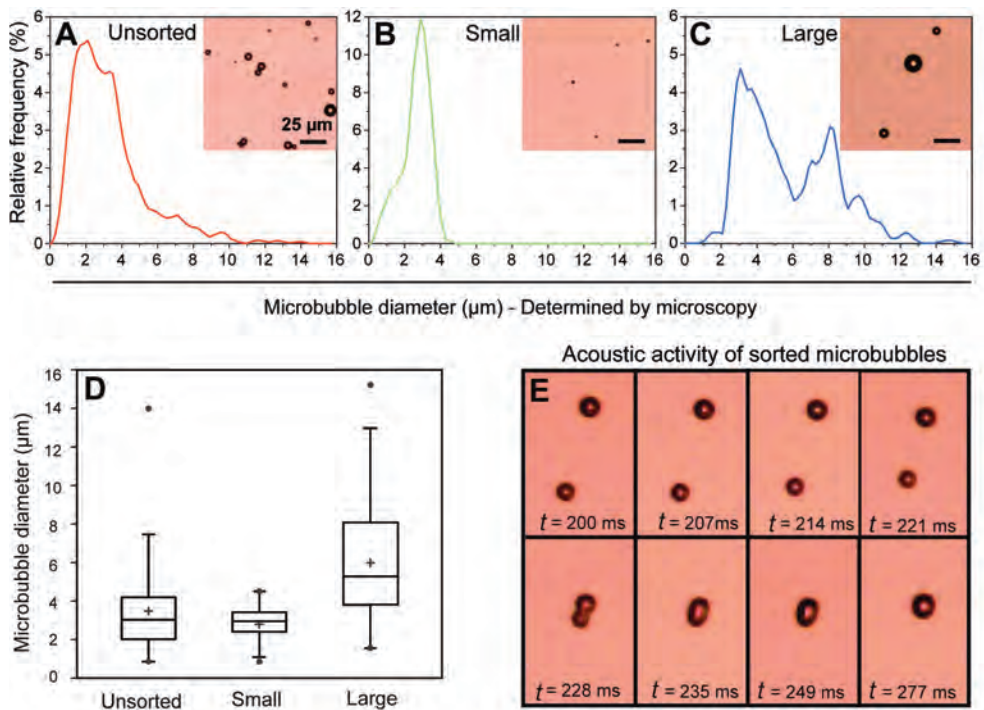

Figure 5 - Flow cytometry assisted particle sorting of microbubbles based on size and fluorescence. (a) Two populations of microbubbles were discriminated based on size and sorted using FACSAria cell sorter. (**A**) Bright field micrograph and a 5-step average smoothened histogram for the sorted microbubbles before sorting; (**B**) Small microbubbles after sorting; (**C**) Large microbubbles after sorting. (**D**) Box plot describing microbubble size distribution before and after size sorting. Cross: mean, Box centre line: median, Box bottom line: 1st quartile, Box top line: 3rd quartile, Bottom and top whiskers: 5th-95th percentiles, Dots: minimum and maximum values. (**E**) Image sequence of large sorted microbubbles under sonication at MI=1.2. Inter-frame time is 7 ms.
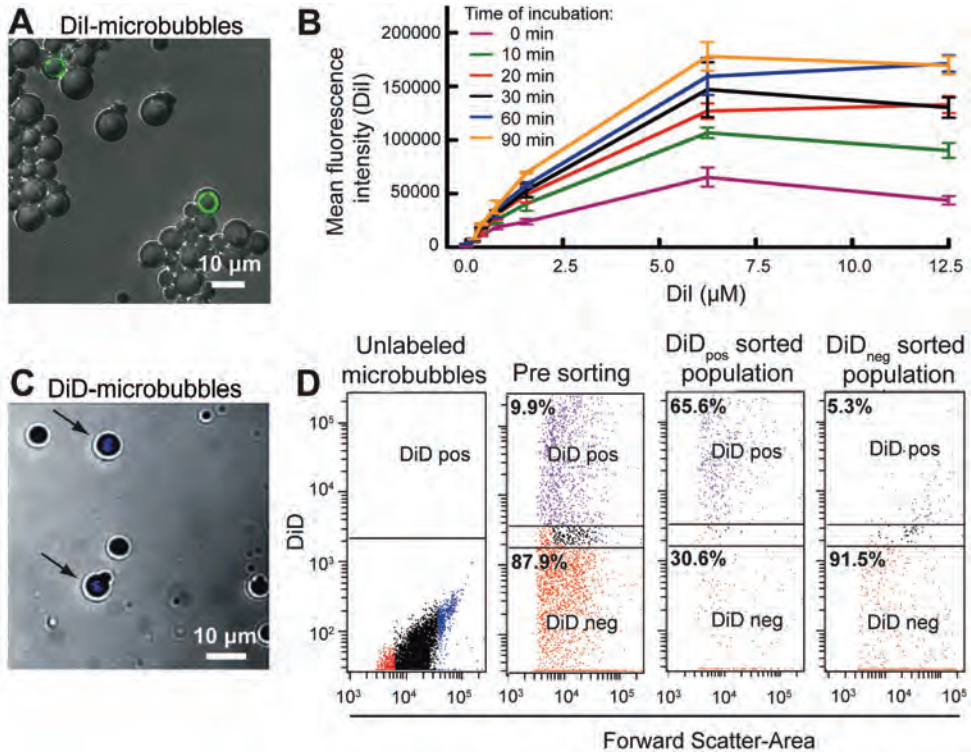
Figure 6 - Screening of fluorescent microbubbles. (**A**) Confocal microscopy (63 x 1.4 oil) of microbubbles illustrating binding of DiI in the lipid membrane of the microbubbles. Scale bar, 10 μm. (**B**) Graph of DiI mean fluorescence intensity illustrating various DiI concentrations stained at different time points (0-90 min). (**C**) Confocal micrograph of DiD labelled microbubbles before sorting (**E**) Flow cytometric analysis of unlabelled microbubbles; DiD labelled microbubbles before sorting; DiD labelled microbubbles sorted for DiD fluorescence; Sorted for no DiD fluorescence.

Discussion

After testing the lipid-shelled microbubbles in multiple flow cytometers with different flow rates and pressures, we observed a similar serpentine scatter pattern indicating that these parameters do not affect the microbubble analysis. This serpentine pattern was not observed in the albumin-shelled microbubbles (Fig. 4), and allowed a clear distinction between the two types of microbubbles. This could be due to the different shell properties, e.g. heterogeneity in shell composition from microbubble to microbubble. This scatter pattern may correlate to different shell stiffness thus be used to evaluate and optimize custom microbubbles. We conclude that microbubble analysis can be performed using a large variety of flow cytometers.

The characteristic serpentine shape and repeatable relative forward/side scatter location of the microbubbles also allowed for distinction of microbubbles in mixture with cell lines or whole blood (Fig. 3). Flow cytometry enabled rapid and accurate measurements of microbubble concentrations. These were in agreement with other concentration measurement methods. The stability of the microbubbles was greatly improved when storing at 4ºC. This could be explained by the lower gas diffusion rate at a lower temperature.

Small microbubbles with a narrow size distribution have the ability to pass capillaries and could be used to improve harmonic imaging [21,26] and to reduce the risk of microbubbles blocking lung capillaries respectively [27]. Particle sorting was used to isolate microbubbles based on particle size or fluorescence emission (Figs. 5 and 6). After sorting, it was seen that the stability of the microbubbles during sonication was decreased indicating that fluorescence-activated sorting alters the microbubble shell. In the control samples microbubbles demonstrated stability for several minutes of sonication, in contrast to sorted microbubbles, which dissolved following less than 10 seconds sonication. The sorted microbubbles demonstrated a higher likelihood of coalescing, indicating a thinner shell that is more susceptible to film drainage [28]. Also, sorting of microbubbles appeared more effective for small bubbles, demonstrating a more uniform size distribution and absence of contamination with large bubbles (Fig. 5 B and C). This contamination may be a consequence of the sorter sensitivity allowing multiple microbubbles per droplet. The droplet formation by the vibrating nozzle could fragment microbubbles. Furthermore the microbubble concentration after sorting was decreased thereby possibly limiting the use of flow cytometry in large scale microbubble sorting. Sorting by size is beneficial as it allows a narrower size distribution at required resonance frequencies.

Fluorescence-based sorting allowed a concentration enhancement of fluorescent microbubbles. Potential uses of this application could be to sort fluorescent drug loaded microbubbles for use in ultrasound-assisted drug delivery and fluorescently labelled functional antibodies attached to microbubbles for use in molecular imaging.

Microbubbles have revolutionized clinical analysis of vascularity and perfusion, and are currently tested as vehicles for drug delivery [12,13]. Our results indicated that flow cytometry is a relatively non-destructive analysis method that can be used to evaluate gas-filled microbubbles. Flow cytometry is an existing technique widely available in research and clinical laboratories and could easily be implemented in current development of functionalized microbubbles for clinical use. We anticipate that flow cytometry can be an important tool to optimize microbubble fabrication for improved contrast-enhanced ultrasonography and microbubble facilitated drug delivery.

Acknowledgments

References

1. *Basic and New Aspects of Gastrointestinal Ultrasonography*, ed. Ødegaard S, Gilja OH, and G. H. Vol. 3. 2005, Singapore: World Scientific. 502.
2. Postema, M. and O.H. Gilja, *Contrast-enhanced and targeted ultrasound.* World J Gastroenterol, 2011. **17**(1): p. 28-41.
3. Postema, M. and O.H. Gilja, *Ultrasound-directed drug delivery.* Curr Pharm Biotechnol, 2007. **8**(6): p. 355-61.
4. Postema, M., *Fundamentals of Medical Ultrasonics* 2011, London: Spon Press.
5. Alexandrov, A.V. et al., *Ultrasound-enhanced systemic thrombolysis for acute ischemic stroke.* N Engl J Med, 2004. **351**(21): p. 2170-8.
6. Klibanov, A.L. et al., *Targeted ultrasound contrast agent for molecular imaging of inflammation in high-shear flow.* Contrast Media Mol Imaging, 2006. **1**(6): p. 259-66.
7. Pysz, M.A. et al., *Antiangiogenic cancer therapy: monitoring with molecular US and a clinically translatable contrast agent (BR55).* Radiology, 2010. **256**(2): p. 519-27.
8. Dijkmans, P.A. et al., *Microbubbles and ultrasound: from diagnosis to therapy.* Eur J Echocardiogr, 2004. **5**(4): p. 245-56.
9. van Wamel, A. et al., *Vibrating microbubbles poking individual cells: drug transfer into cells via sonoporation.* J Control Release, 2006. **112**(2): p. 149-55.
10. Schneider, M., *Molecular imaging and ultrasound-assisted drug delivery.* J Endourol, 2008. **22**(4): p. 795-802.
11. Klibanov, A.L., *Microbubble contrast agents: targeted ultrasound imaging and ultrasound-assisted drug-delivery applications.* Invest Radiol, 2006. **41**(3): p. 354-62.
12. Bull, J.L., *The application of microbubbles for targeted drug delivery.* Expert Opin Drug Deliv, 2007. **4**(5): p. 475-93.
13. Mitragotri, S., *Healing sound: the use of ultrasound in drug delivery and other therapeutic applications.* Nat Rev Drug Discov, 2005. **4**(3): p. 255-60.
14. Delalande, A. et al., *Ultrasound and microbubble-assisted gene delivery in Achilles tendons: Long lasting gene expression and restoration of fibromodulin KO phenotype.* J Control Release, 2011. 156(2): p. 223-230.
15. Bao, S., B.D. Thrall, and D.L. Miller, *Transfection of a reporter plasmid into cultured cells by sonoporation in vitro.* Ultrasound Med Biol, 1997. **23**(6): p. 953-9.
16. Prentice P, C.A., Dholakia K, Prausnitz M and Campbell P, *Membrane disruption by optically controlled microbubble cavitation.* Nature Physics, 2005. **1**: p. 107 - 110.
17. Stringham, S.B. et al., *Over-pressure suppresses ultrasonic-induced drug uptake.* Ultrasound Med Biol, 2009. **35**(3): p. 409-15.
18. Schlicher, R.K. et al., *Mechanism of intracellular delivery by acoustic cavitation.* Ultrasound Med Biol, 2006. **32**(6): p. 915-24.